BBA - Molecular Basis of Disease 1865 (2019) 1490–1501

Contents lists available at ScienceDirect

BBA - Molecular Basis of Disease

journal homepage: www.elsevier.com/locate/bbadis

Reduced biliverdin reductase-A levels are associated with early alterations of insulin signaling in obesity

Flavia Agata Cimini[a,1], Andrea Arena[b,1], Ilaria Barchetta[a,1], Antonella Tramutola[b], Valentina Ceccarelli[a], Chiara Lanzillotta[b], Mario Fontana[b], Laura Bertoccini[a], Frida Leonetti[a], Danila Capoccia[a], Gianfranco Silecchia[c], Claudio Di Cristofano[c], Caterina Chiappetta[c], Fabio Di Domenico[b], Marco Giorgio Baroni[a], Marzia Perluigi[b], Maria Gisella Cavallo[a,*], Eugenio Barone[b,**]

[a] Department of Experimental Medicine, Sapienza University of Rome, Rome, Italy
[b] Department of Biochemical Sciences "A. Rossi-Fanelli" Sapienza University of Rome, Rome, Italy
[c] Department of Medical-Surgical Sciences and Bio-Technologies, Sapienza University of Rome, Rome, Italy

ARTICLE INFO

Keywords:
Biliverdin reductase-a
Obesity
Insulin signaling
Metabolic disorders

ABSTRACT

Biliverdin reductase-A (BVR-A) is a serine/threonine/tyrosine kinase involved in the regulation of insulin signaling. *In vitro* studies have demonstrated that BVR-A is a substrate of the insulin receptor and regulates IRS1 by avoiding its aberrant activation, and in animal model of obesity the loss of hepatic BVR-A has been associated with glucose/insulin alterations and fatty liver disease. However, no studies exist in humans. Here, we evaluated BVR-A expression levels and activation in peripheral blood mononuclear cells (PBMC) from obese subjects and matched lean controls and we investigated the related molecular alterations of the insulin along with clinical correlates. We showed that BVR-A levels are significantly reduced in obese subjects and associated with a hyper-activation of the IR/IRS1/Akt/GSK-3β/AS160/GLUT4 pathway. Low BVR-A levels also associate with the presence of obesity, metabolic syndrome, NASH and visceral adipose tissue inflammation. These data suggest that the reduction of BVR-A may be responsible for early alterations of the insulin signaling pathway in obesity and in this context may represent a novel molecular target to be investigated for the comprehension of the process of insulin resistance development in obesity.

1. Introduction

Obesity is a constantly increasing clinical condition that represents one of the greatest public health epidemics of our century and it is associated with numerous cardiovascular disease risk factors, such as metabolic syndrome (MS), type 2 diabetes (T2D) and non-alcoholic fatty liver disease (NAFLD) [1]. Molecular mechanisms driving the metabolic alterations in obesity are only partially understood and, in this context, insulin resistance has been suggested as one of the key elements [2,3]. Despite the bulk of data on causes and consequences of insulin resistance, the molecular mechanisms behind the development of impaired insulin in obesity have not been completely elucidated, yet.

The insulin cascade contains several regulatory steps, which represent critical nodes [4]. Among them, biliverdin reductase-A (BVR-A) recently emerged for its pleiotropic functions. BVR-A is an evolutionary conserved enzyme ubiquitously expressed [5–7]. BVR-A is mainly known for its activity in the degradation pathway of heme where BVR-A reduces heme oxygenase (HO)-derived biliverdin into bilirubin, this latter being one of the stronger endogenous antioxidant [5–7]. For that reason, BVR-A has been studied for a long time as antioxidant enzyme able to confer cytoprotection against oxidative stress-induced alterations [5,6,8,9]. Interestingly, during the last years, BVR-A has been demonstrated to be endowed with a serine/threonine/tyrosine (Ser/Thr/Tyr) kinase activity directly involved in the regulation of insulin at different levels [10,11]. Indeed, like the insulin receptor substrate-1 (IRS1), BVR-A is a direct target of the insulin receptor (IR),

* Correspondence to: M.G. Cavallo, Department of Experimental Medicine, Section of Medical Pathophysiology, Food Science and Endocrinology, Viale del Policlinico 155, 00161 Rome, Italy.
** Correspondence to: E. Barone, Department of Biochemical Sciences "A. Rossi-Fanelli", Sapienza University of Rome, Piazzale A. Moro 5, 00185 Rome, Italy.
E-mail addresses: gisella.cavallo@uniroma1.it (M.G. Cavallo), eugenio.barone@uniroma1.it (E. Barone).
[1] These authors equally contributed to this work.

https://doi.org/10.1016/j.bbadis.2019.02.021
Received 7 January 2019; Received in revised form 11 February 2019; Accepted 26 February 2019
Available online 28 February 2019
0925-4439/

which phosphorylates both BVR-A and IRS1 on specific Tyr residues thus resulting in their activation [10]. IRS1 mediates the activation of the phosphatidil insositol 3-kinase/protein kinase B (PI3K/Akt), which favors the translocation of the glucose transporter type 4 (GLUT4) to the plasma membrane to mediate glucose uptake. In parallel, BVR-A acts by phosphorylating IRS1 on Ser residues – *i.e.*, Ser307 acting as inhibitory site [10] – to avoid an excessive activation of IRS1, thus representing an upstream regulator of the entire insulin cascade. Furthermore, downstream IR/IRS1, BVR-A favors the PDK1-mediated activation of Akt [12].

Although several reports both form our group and others demonstrated the role of BVR-A in the insulin cascade *in vitro* [10–16], only few studies on metabolic disorders are available *in vivo* [17,18] and no evidence exists in humans. Loss of hepatic BVR-A has been associated with altered metabolic profile in mice [18]. In particular, liver-specific knock-out (KO) mice for BVR-A, fed with high fat diet, developed worse glucose/insulin regulation and more severe hepatic steatosis than wild type [18]. Similarly, kidney-specific KO mouse at the level of proximal tubules were characterized by increased level of lipid accumulation [17], thus implying that BVR-A is part of critical survival pathways including insulin.

Based on these lines of evidence, aim of this study was to evaluate BVR-A levels and its activation state as protein kinase (thereafter BVR-A activation) a in peripheral blood mononuclear cells (PBMC) from obese subjects and lean matched controls to investigate the related molecular alterations in insulin and how they were associated with clinical correlates.

2. Methods

2.1. Study population

For this study, we recruited twenty consecutive obese individuals referring to the Diabetes and Endocrinology outpatient clinics of Sapienza University, Rome, Italy, for metabolic characterization and twenty age- and gender-matched non-obese healthy subjects, as a control group. All the study participants underwent complete clinical workup including medical history collection, clinical examination, anthropometric measurements and laboratory tests (Tables 1 and 2). Weight, height and waist circumference were measured, and body mass index calculated [BMI; weight (kg) x squared height (m^2)]; systemic systolic (SBP) and diastolic (DBP) blood pressure were assessed after 5 min resting and mean values of three consecutive assessments were recorded. Overnight fasting blood samples were obtained in all the study participants for routine biochemistry and to collect peripheral blood mononuclear cells (PBMC). Fasting blood glucose (FBG, mg/dL), glycosylated hemoglobin (HbA1c, % - mmol/mol), total cholesterol (mg/dL), high-density lipoprotein cholesterol (HDL, mg/dL), triglycerides (mg/dL), aspartate aminotransferase (AST, IU/L), alanine aminotransferase (ALT, IU/L) and creatinine (mg/dL) were measured by centralized standard methods. Low-density lipoprotein (LDL) cholesterol value was calculated by the Friedwald formula. The presence of MS was defined by the modified NCEP ATP-III criteria (Grundy SM). Obese subjects underwent oral glucose tolerance test (OGTT), measuring blood glucose (BG, mg/dL) and insulin values (BI, μU/mL) before and 30, 60, 90, and 120 min after glucose load (75 g). Insulin resistance and secretion were estimated by calculating the main static and OGTT-derived indexes, such as the Homeostasis Model Assessment of Insulin Resistance (HOMA-IR, FBG*FBI22,5) [19], the Matsuda sensitivity index (ISI, 10000/(FBG*FBI*BG_{mean}*BI_{mean}) [19], the corrected insulin response (CIR, 100*BI_{30}/[BG_{30}*(BG_{30}–3.89)] [20] and the Disposition index (DI, ISI * CIR) [21]. Within the obese cohort, fifteen subjects underwent bariatric surgery for clinical purposes. The presence of MS was defined by the modified NCEP ATP-III criteria (Grundy SM). The diagnosis of NAFLD and NASH was performed on liver biopsies based on Brunt criteria [22,23]; the presence of signatures of VAT inflammation was investigated on VAT biopsies obtained intra-operatively, by immunohistochemistry and gene expression, as previously described [24].s The study protocol was reviewed and approved by the Ethics Committee of Policlinico Umberto I, Sapienza University of Rome and conducted in conformance with the Helsinki Declaration. Written consent was obtained from all patients before the study.

Table 1
Clinical and biochemical characteristics of obese individuals and controls. * Pearson's Chi-squared test applied.

	Obese subjects (n = 20)	Controls (n = 20)	P-value
Age (years)	40.7 ± 9.1	46.5 ± 12.6	0.06
Gender (M%)	7/13	5/15	0.33*
BMI (Kg/m^2)	42.8 ± 4.8	23.3 ± 2.7	< 0.001
Body weight (kg)	114.7 ± 15.4	65.3 ± 12	< 0.001
Waist circumference (cm)	128.9 ± 10.9	83.2 ± 11	< 0.001
SBP (mmHg)	127.3 ± 20.4	116 ± 15.6	0.06
DBP (mmHg)	80.6 ± 5.8	75 ± 10.9	0.07
Total cholesterol (mg/dl)	195.4 ± 28.1	184 ± 54.3	0.43
HDL-C (mg/dl)	46.4 ± 11.5	64.9 ± 16.2	< 0.001
LDL-C (mg/dl)	121.2 ± 22–6	101.4 ± 44.3	0.10
Triglycerides (mg/dl)	138.9 ± 35	134 ± 43.1	< 0.001
FBG (mg/dl)	94.1 ± 12.4	87.9 ± 8.25	0.09
AST (IU/l)	25.3 ± 11.4	21 ± 6.4	0.20
ALT (IU/l)	30.6 ± 16.1	21.5 ± 9.3	0.06
MS (yes/no)	95%	0%	< 0.001*
MS (# components)	0 = 0%	0 = 90%	< 0.001*
	1 = 0%	1 = 0%	
	2 = 5%	2 = 10%	
	3 = 5%	3 = 0%	
	4 = 74%	4 = 0%	
	5 = 16%	5 = 0%	
BVR-A	38.7 ± 29.3	100 ± 36.7	< 0.001

Table 2
Metabolic characteristics of obese subjects.

Parameters	Obese subjects (n = 20)
BG 0′	94.1 ± 12.4
BG 30′	152.7 ± 30.1
BG 60′	155.7 ± 27.4
BG 90′	142.6 ± 31.8
BG 120′	123.7 ± 18.3
BI 0′	15.4 ± 12.7
BI 30′	81.1 ± 113.4
BI 60′	84.7 ± 120.8
BI 90′	104.1 ± 184.3
BI 120′	81.7 ± 97.6
MS	95%
HOMA-IR	3.7 ± 3.4
HOMA-β	186.9 ± 41.3
DI	14,805.7 ± 26,340.3
CIR 30	312.6 ± 190.8
ISI	66.9 ± 83.5

2.2. Samples collection

PBMC are increasingly used as surrogate model for glucose disposal. Recent studies have shown that PBMC have insulin-sensitive GLUT4 activity and that GLUT4 increases on the membrane of monocytes [25–27] and lymphocytes [28,29] in response to insulin. Furthermore, BVR-A expression is consistent in PBMC [30,31]. In addition, PBMC are easy to collect repeatedly in sufficient quantities [32–34]. As a whole, PBMC could potentially serve as a proxy tissue [25,27] allowing sampling of large study population and making the procedures necessary for research less invasive. The use of PBMC is therefore of help to perform cellular-based studies aimed to compare changes in obese

subjects with respect to matched controls, which otherwise would be not possible.

PBMC were isolated from overnight fasting blood samples. ACD-A-anticoagulated blood was centrifuged at 800 ×*g* for 30 min and the top layer containing plasma was removed. The remaining blood was diluted with an equal volume of phosphate-buffered saline, pH 7.4 (PBS), containing 0.05 M ethylenediaminetetraacetic acid (EDTA; Invitrogen). 12.5 ml of diluted blood was layered over 25 ml of the Ficoll-Paque PLUS (GE Healthcare). Gradients was centrifuged at 400 ×*g* for 30 min at room temperature in a swinging-bucket rotor without the brake applied. The PBMC interface was carefully removed by pipetting and washed with PBS-EDTA by centrifugation at 250 ×*g* for 10 min. PBMC pellets were suspended in ammonium-chloride-potassium (ACK) lysing buffer (Invitrogen) and incubated for 10 min at room temperature with gentle mixing to lyse contaminating red blood cells (RBC), then washed with PBS-EDTA. Cell number and viability were determined using a Countess Automated Cell Counter (Invitrogen). Non-viable cells were identified by staining with trypan blue and cell viability was calculated using the total cell count and the count of non-viable cells. PBMC were cryopreserved in liquid nitrogen in fetal calf serum (FCS; Invitrogen) containing 10% dimethyl sulfoxide (DMSO; Thermo Fisher Scientific) and stored until required for downstream analyses.

2.3. Samples preparation

Total protein extracts were prepared in RIPA buffer (pH 7.4) containing Tris-HCl (50 mM, pH 7.4), NaCl (150 mM), 1% NP-40, 0.25% sodium deoxycholate, EDTA (1 mM), 0.1% SDS, supplemented with proteases inhibitors [phenylmethylsulfonyl fluoride (PMSF, 1 mM), sodium fluoride (NaF, 1 mM) and sodium orthovanadate (Na_3VO_4, 1 mM)]. PBMC were homogenized by 20 passes with a Wheaton tissue homogenizer and then clarified by centrifugation for 1 h at 16,000 ×*g*, 4 °C. The supernatant was then extracted to determine the total protein concentration by the Bradford assay (Pierce, Rockford, IL).

2.4. RNA extraction and quantitative real-time RT-PCR

RNA was extracted from the PBMC in all groups (n = 20/group) using Tissue Total RNA Kit according to manufacturer's instructions (Fisher Molecular biology, Rome, Italy). RNA was quantified using the Biospec Nano spectrophotometer (Shimadzu, Columbia, MD, USA), and RNA was reverse transcribed using the cDNA High Capacity kit (Applied Biosystems, Foster City, CA, USA), including reverse transcriptase, random primers and buffer according to manufacturer's instructions. The cDNA was produced through a series of heating and annealing cycles in the MultiGene OPTIMAX 96-well Thermocycler (LabNet International, Edison, NJ, USA). The primers used for evaluation of BVR-A gene expression are: Fw 5′-CGAAGGAAGAGACCAAGAT GAA-3′ and Rv 5′-GGAAAGAGCATCCTCCAAAGA-3′. Real time PCR (Q-PCR) was performed using the following cycling conditions: 35 cycles of denaturation at 95 °C for 20 s; annealing and extension at 60 °C for 20 s, using the SensiFAST™ SYBR® No-ROX Kit (Bioline, London, UK). PCR reactions were carried out in a 20 μl reaction volume in a CFX Connect Real Time PCR machine (Bio-Rad Laboratories, Hercules, CA, USA). Relative mRNA concentrations were calculated from the take-off point of reactions (threshold cycle, Ct) using the comparative quantitation method performed by Bio-Rad software and based upon the −ΔΔCt method. Ct values for GAPDH expression (Fw 5′-GACAGTCAGCCGCA TCTTCT-3′ and Rv 5′- TTAAAAGCAGCCCTGGTGAC-3′) served as a normalizing signal (REF. Livak KJ, Schmittgen TD). Analysis of relative gene expression data using real-time quantitative PCR and the 2(T) (−Delta Delta C) method [35].

2.5. Western blot

For western blots, 30 μg of proteins were resolved on 12% and 7.5% SDS–PAGE using Criterion Gel TGX (Bio-Rad, Hercules, CA, USA). Before immunoblot analysis the gel image analyzed for total protein load was acquired to then normalize blot analysis. For immunoblot analysis, gels were transferred onto nitrocellulose membranes (Bio-Rad, Hercules, CA, USA) and membranes were blocked with 3% bovine serum albumin in 0.5% Tween-20/Tris-buffered saline (TTBS) and incubated overnight at 4 °C with the following antibodies: anti-BVR-A (1:1000, Sigma-Aldrich, St Louis, MO, USA, #B8437), anti-phospho (Tyr198)-BVR-A (1:500, Biomatick, Wilmington, DL, USA, #SA170103), anti-IRβ (1:1000, Cell Signaling, Bioconcept, Allschwill, Switzerland, #3020), anti-phospho(Tyr1158/1162/1163)-IRβ (1:1000, Genetex, Irvine, CA, USA, #GTX25681), anti-IRS1 (1:1000, Cell Signaling, Bioconcept, Allschwill, Switzerland, #3407), anti-phospho (Ser307)-IRS1 (1:500, Cell, Bioconcept, Allschwill, Switzerland, #2381), anti-phospho(Tyr632)-IRS1 (1:500, Santa Cruz, Santa Cruz, CA, USA, #sc-17,196), anti-Akt (1:1000, Cell Signaling, Bioconcept, Allschwill, Switzerland, #11E7), anti-phospho(Ser473)-Akt (1:1000, Cell Signaling, Bioconcept, Allschwill, Switzerland, #193H12), anti-GSK-3β (1:1000, Santa Cruz, Santa Cruz, CA, USA, #sc-377213), anti-phospho(Ser9)-GSK-3β (1:500, Santa Cruz, Santa Cruz, CA, USA, #sc-373800), anti-phospho(Tyr216)-GSK-3β (1:500, Santa Cruz, Santa Cruz, CA, USA, #sc-135653), anti-mTOR (1:1000, Cell Signaling, Bioconcept, Allschwill, Switzerland, #2983), anti-phospho(Ser2448)-mTOR (1:500, Cell Signaling, Bioconcept, Allschwill, Switzerland, #5536), anti-GLUT4 (1:1000, Santa Cruz, Santa Cruz, CA, USA, #sc-53566), anti-AS160 (1:1000, Thermo Fischer, Waltham, MA, USA), anti-phospho(Thr642)-AS160 (1:1000, GeneTex, Irvine, CA, USA). After 3 washes with TTBS the membranes were incubated for 60 min at room temperature with anti-rabbit/mouse/goat IgG secondary antibody conjugated with horseradish peroxidase (1:5000; Sigma–Aldrich, St Louis, MO, USA). Membranes were developed with the Super Signal West Pico chemiluminescent substrate (Thermo Scientific, Waltham, MA, USA), acquired with Chemi-Doc MP (Bio-Rad, Hercules, CA, USA) and analyzed using Image Lab software (Bio-Rad, Hercules, CA, USA) that permits the normalization of a specific protein signal with the β-actin signal in the same lane or total proteins load.

2.6. Statistics

SPSS version 23 (IBM, Armonk, NY) was used to perform all the statistical analyses. Continuous variables are reported as the mean ± SD and categorical variables as percentages. Clinical parameters which were non–normally distributed underwent log-transformation before the analyses. Comparisons between two groups were performed by Student *t*-test for independent samples and by Pearson χ^2 and Fisher test for categorical variables. Bivariate correlation analyses were calculated by Pearson and Spearman's rank correlations. The predictive value of BVR-A levels for obesity was estimated by the area under receiver-operating characteristic curve (AUROC), with a 95% confidence interval (C.I.). A p value < .05 was considered statistically significant.

3. Results

3.1. Reduced BVR-A protein levels in PBMC from obese subjects

To test the hypothesis that obesity and MS are associated with impaired BVR-A levels/activation, we evaluated changes of BVR-A (i) mRNA and protein levels, (ii) Tyr198 phosphorylation and (iii) the relative p^{Tyr198}BVR-A/BVR-A ratio (as index of protein activation) in PBMC from obese patients compared to lean subjects. The obese subgroup showed around 50% reduction of BVR-A mRNA levels (p = .045, Fig. 1C) and a 60% reduction in BVR-A protein levels (p < .0001, Fig. 1D). Furthermore, we observed 35% reduction of p^{Tyr198}BVR-A (p = .032, Fig. 1E), which is one of the sites of IR-mediated BVR-A phosphorylation [10]. When we evaluated the relative active form

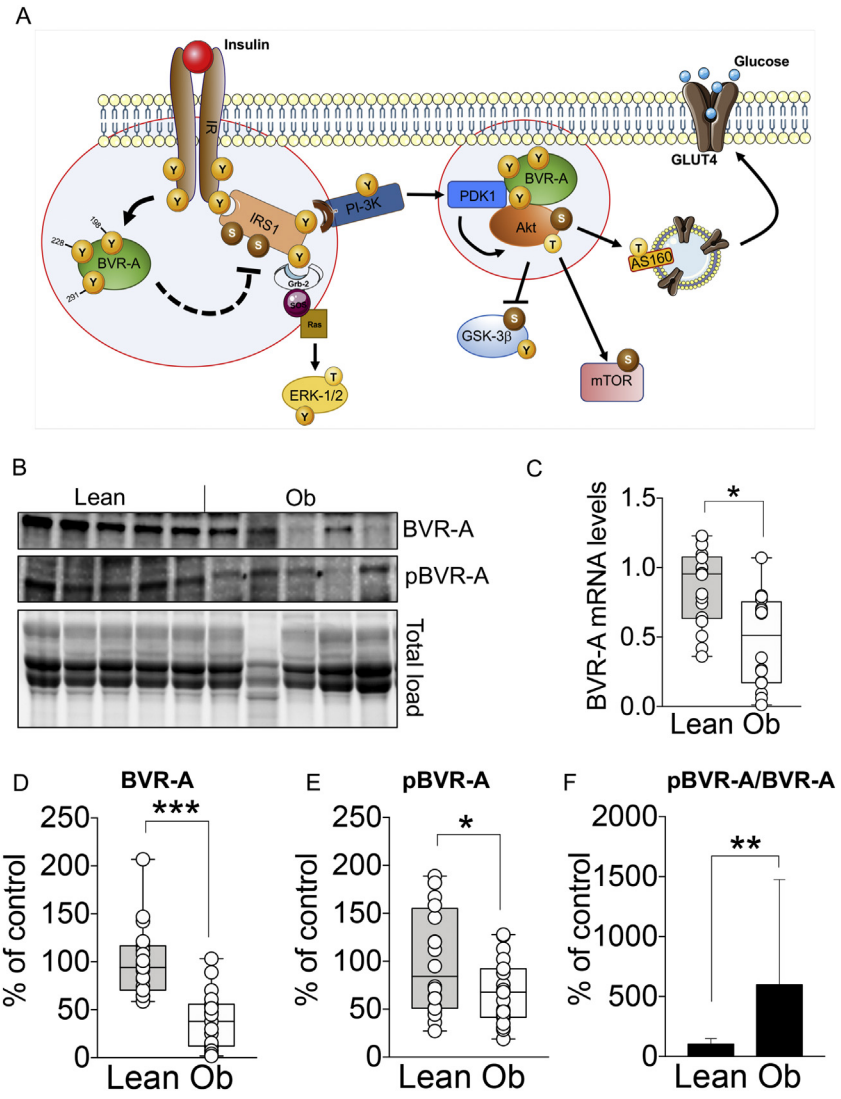

Fig. 1. Reduced BVR-A levels in PBMC from obese individuals. (A) Schematic representation of the insulin cascade with highlighted the critical nodes regulated by BVR-A. Arrows: activation; dotted lines: inhibition; Y: tyrosine residues; S: serine residues. (B) Western blot from lean and obese (Ob) individuals PBMC extracts. Representative gels are shown; (C) BVR-A mRNA levels; (D and E) densitometric evaluation of BVR-A protein levels and BVR-A Tyr198 phosphorylation; (F) BVR-A relative activation expressed as p^{Tyr198}BVR-A/BVR-A ratio. Both total protein levels and respective phosphorylated form were normalized per total protein load. Densitometric values are given as percentage of lean controls set as 100%. Data are presented as means ± SD (n = 20/group). *t*-test, *p < .05, **p < .01, ***p < .001.

(p^{Tyr198}BVR-A) with respect to total protein levels in each subgroup, we found that the p^{Tyr198}BVR-A/BVR-A ratio was significantly higher in obese patients than controls (~400%, p = .018, Fig. 1F).

3.2. Hyper-activation of insulin signaling pathway in PBMC from obese subjects

In order to understand whether changes of BVR-A impact the activation of insulin signaling pathway, we evaluated protein levels and activation state of several of the main components of insulin in PBMC from obese and control subjects. We found no significant changes in IR protein levels and activation (Fig. 2B–D). Downstream IR, a reduction of IRS1 protein levels (~30%, p = .017, Fig. 2E) along with reduced levels of IRS1 inhibitory phosphorylation (p^{Ser307}IRS1) (~40%, p = .003, Fig. 2G) without changes of IRS1 activatory phosphorylation (p^{Tyr632}IRS1) levels (Fig. 2F) in obese subjects with respect to lean controls, were observed. The evaluation of both the active and inactive forms, with respect to total IRS1 protein levels in each subgroup, showed no changes for p^{Tyr632}IRS1/IRS1 (Fig. 2H), while a significant reduction was observed for p^{Ser307}IRS1/IRS1 (~40%, p = .05, Fig. 2I) in obese subjects. At the net of these changes, the ratio between the relative IRS1 activation with respect to its relative inactivation [(p^{Tyr632}IRS1/IRS1)/(p^{Ser307}IRS1/IRS1), *i.e.*, Tyr632/Ser307] revealed that IRS1 was more activated in PBMC from obese patients than lean controls (~200%, p = .019, Fig. 2L). Considering that BVR-A Tyr198 and IRS1 Tyr632 are both targets of IR kinase activity [10,36], we normalized both the relative BVR-A and IRS1 activation with respect to those of IR. We found significantly greater IR-mediated BVR-A (p^{Tyr198}BVR-A/pIR) and IRS1 (p^{Tyr632}IRS1/pIR) activation in obese patients than lean controls (Fig. 2M and N, respectively); thus, we observed a 5-fold increase of IR-mediated BVR-A activation (p = .02, Fig. 2M), while IR-mediated IRS1 activation was almost doubled (p = .02, Fig. 2N). Changes of BVR-A and IRS1 are reflected on the downstream targets and especially on the Akt/GSK-3β axis. PBMC from obese patients had reduced levels of both Akt protein (~70%, p < .001, Fig. 3B) and Akt activatory phosphorylation (p^{Ser473}Akt, ~60%, p < .001, Fig. 3C), although the Akt relative activation (p^{Ser473}Akt/Akt) appears significantly increased (~70%, p = .03, Fig. D). Two of the main targets of Akt are GSK-3β and mTOR [37]. GSK-3β is a constitutively activated protein, which is inhibited following Akt activation [38], while mTOR is activated by Akt [39]. GSK-3β protein levels were reduced in PBMC from obese patients with respect to lean control (~60%, p < .001, Fig. 3E). In agreement with the proposed Akt hyper-activation, we found that GSK-3β activatory phosphorylation (p^{Tyr216}GSK-3β) levels were reduced (~50%, p < .001, Fig. 3F), whereas GSK-3β inhibitory phosphorylation (p^{Ser9}GSK-3β) levels were increased (~30%, p = .04, Fig. 3G) in obese patients compared to lean controls. Both the relative GSK-3β activation (p^{Tyr216}GSK-3β/GSK-3β, p = .01) and inactivation (p^{Ser9}GSK-3β/GSK-3β, p = .01) were significantly increased (Fig. 3H and I, respectively). However, the ratio

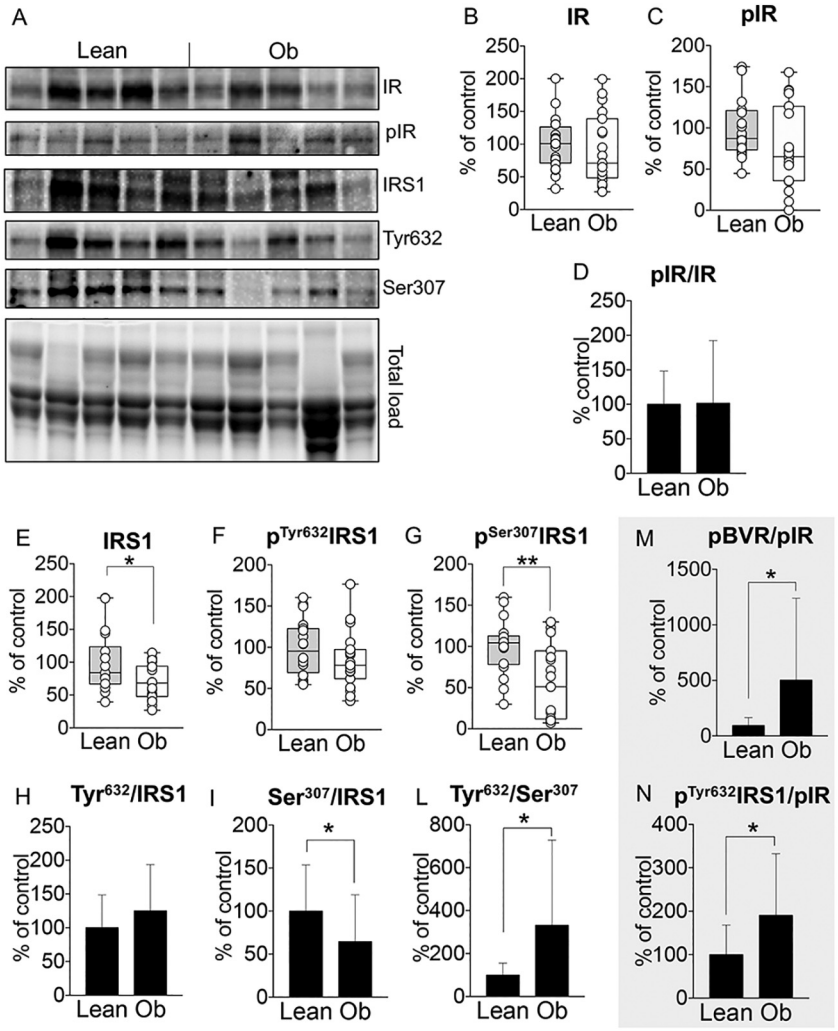

Fig. 2. IRS1 hyper-activation in PBMC from obese individuals. (A) Western blot from lean and obese (Ob) individuals PBMC extracts. Representative gels are shown; (B) densitometric evaluation of IR protein levels; (C) densitometric evaluation of $p^{Tyr1158/1162/1163}$IR levels; (D) IR relative activation expressed as $p^{Tyr1158/1162/1163}$IR/IR ratio; (E) densitometric evaluation of IRS1 protein levels; (F) densitometric evaluation of p^{Tyr632}IRS1 levels; (G) densitometric evaluation of p^{Ser307}IRS1 levels; (H) IRS1 relative activation evaluated as p^{Tyr632}IRS1/IRS1 ratio; (I) IRS1 relative inactivation evaluated as p^{Ser307}IRS1/IRS1; (L) IRS1 activation/inactivation ratio evaluated as (p^{Tyr632}IRS1/IRS1)/(p^{Ser307}IRS1/IRS1); (M) BVR-A activation normalized with respect IR activation expressed as p^{Tyr198}BVR-A/BVR-A)/($p^{Tyr1158/1162/1163}$IR/IR) ratio; (N) IRS1 activation normalized with respect IR activation expressed as (p^{Tyr632}IRS1/IRS1)/($p^{Tyr1158/1162/1163}$IR/IR). Both total protein levels and respective phosphorylated forms were normalized per total protein load. Densitometric values are given as percentage of lean controls set as 100%. Data are presented as means s ± SD (n = 20/group). *t*-test, *p < .05, **p < .01.

between the relative GSK-3β activation and inactivation [(p^{Tyr216}GSK-3β/GSK-3β)/(p^{Ser9}GSK-3β/GSK-3β)] resulted in a significant decrease of GSK-3β activation (~50%, p < .0001, Fig. 3L). No changes were observed for mTOR (Fig. 3M–O).

3.3. Increased GLUT4 protein levels and translocation in PBMC from obese subjects

To explore whether the observed hyper-activation of insulin cascade resulted in changes of levels and translocation at the plasma membrane of the insulin-sensitive glucose transporter GLUT4, we evaluated protein levels and activation of AS160 (known to mediate GLUT4 translocation [40]), as well as total GLUT4 protein levels. We found 50% reduction of AS160 protein levels (p < .01, Fig. 4B) along with a significant increase (~80%, p < .05, Fig. 4C) of AS160 active form (p^{Thr642}AS160), finally resulting in a significant increase of the relative AS160 activation as evaluated as p^{Thr642}AS160/AS160 ratio (~300%, p < .001, Fig. 4D) in PBMC from obese patients with respect to lean controls. In parallel, a significant increase of GLUT4 protein levels (~25%, p = .02, Fig. 4E) was observed.

3.4. Association between reduced BVR-A protein levels and the hyper-activation of the insulin in obese subjects

To support the hypothesis that a reduction of BVR-A protein levels favors the hyper-activation of the insulin- cascade in obese patients, we evaluated the existence of a possible direct association between BVR-A protein levels and the activation of the insulin- cascade. In particular, we looked upstream at the IR-mediated activation of BVR-A and IRS1, while downstream at the expression of GLUT4 and at the activation of AS160 as final events associated with the activation of the insulin-cascade in PBMC. We confirmed that BVR-A protein levels negatively correlated with both IR-mediated (i) BVR-A activation (r = −0.61, p = .0001, Fig. 4F) and (ii) IRS1 activation (r = −0.35, p = .037, Fig. 4G). In line with that, a positive correlation between BVR-A protein levels and p^{Ser307}IRS1 levels was found (r = 0.45, p = .005, Fig. 4H). In addition, significant negative correlations were observed between BVR-A protein levels and both AS160 activation (r = −0.42, p = .01, Fig. 4I) and GLUT4 protein levels (r = −0.33, p = .04, Fig. 4L). Furthermore, the sustained activation of both BVR-A and IRS1 was positively associated with GLUT4 levels [for p^{Tyr}BVR-A/pIR: r = 0.56, p = .0008 Fig. 4M; for p^{Tyr}IRS1/pIR: r = 0.3, p = .07, Fig. 4N] and AS160 activation [for p^{Tyr}IRS1/pIR: r = 0.38, p = .04, Fig. 4O], thus suggesting that to a reduction of BVR-A protein levels corresponds a hyper-activation of the insulin cascade. This hyper-activation is characterized an increased activation IRS1, which finally results in an increased translocation of GLUT4 at the plasma membrane. In parallel, the increased IR-mediated activation of BVR-A suggest that cells try to compensate the consistent loss of BVR-A protein by promoting BVR-A phosphorylation. However, this seems not enough to prevent the hyper-activation of the signal.

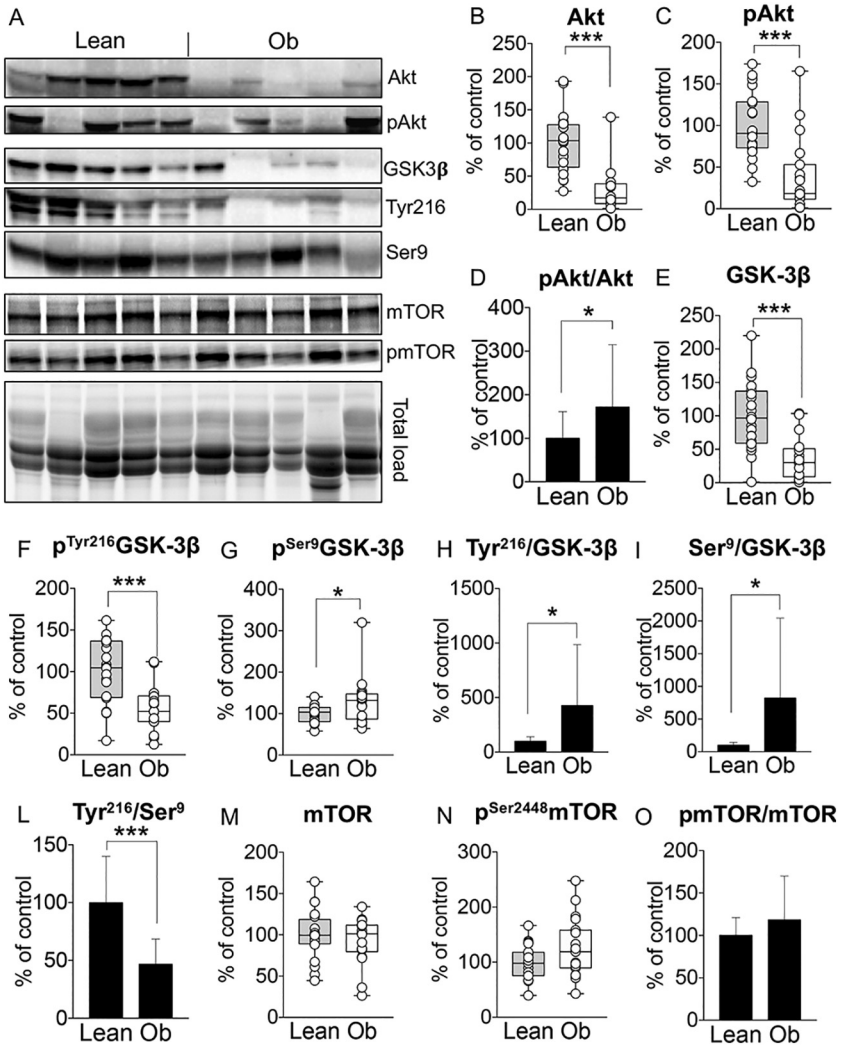

Fig. 3. Akt/GSK-3β axis hyper-activation in PBMC from obese individuals. (A) Western blot from lean and obese (Ob) individuals PBMC extracts. Representative gels are shown; (B) densitometric evaluation of Akt protein levels; (C) densitometric evaluation of p^{Ser473}Akt levels; (D) Akt relative activation expressed as p^{Ser473}Akt/Akt ratio; (E) densitometric evaluation of GSK-3β protein levels; (F) densitometric evaluation of p^{Tyr216}GSK-3β levels; (G) densitometric evaluation of p^{Ser9} GSK-3β levels; (H) GSK-3β relative activation evaluated as p^{Tyr216}GSK-3β/GSK-3β ratio; (I) GSK-3β relative inactivation evaluated as p^{Ser9}GSK-3β/GSK-3β; (L) GSK-3β activation/inactivation ratio evaluated as (p^{Tyr216}GSK-3β/GSK-3β)/(p^{Ser9}GSK-3β/GSK-3β); (M) densitometric evaluation of mTOR protein levels; (N) densitometric evaluation of $p^{Ser2448}$mTOR levels; mTOR relative activation expressed as $p^{Ser2448}$mTOR/mTOR ratio. Both total protein levels and respective phosphorylated forms were normalized per total protein load. Densitometric values are given as percentage of lean controls set as 100%. Data are presented as means ± SD (n = 20/group). *t*-test, *p < .05, ***p < .001.

3.5. BVR-A and clinical evaluations

When exploring possible clinical determinants of altered BVR-A in the overall population (clinical and biochemical parameters of the study population are showed in Tables 1 and 2), we observed that lower BVR-A protein levels were associated with the presence of obesity ($r = -0.65$, $p = .1$), greater BMI ($r = -0.62$, $p < .001$), body weight ($r = -0.5$, $p < .001$) and waist circumference ($r = -0.57$, $p < .001$), and with the presence and number of components of MS ($r = -0.68$, $p < .001$; ($r = -0.70$, $p < .001$). Reduced BVR-A protein levels identified obesity with AUROC = 0.93 (95%C.I.: 0.85–1.00, $p < .001$), sensitivity = 0.84 and specificity = 0.84 for BVR-A protein levels ≤64.4 (Fig. 5). We also showed that, in obese subjects, BVR-A protein levels were negatively associated with the AUC OGTT ($r = -0.57$, $p = .015$) but positively with CIR30 ($r = 0.64$, $p = .006$) and with DI ($r = 0.62$, $p = .01$). No correlation was found with HOMA-IR and ISI.

3.6. Association between BVR-A protein levels and NAFLD/NASH and visceral adipose tissue (VAT) inflammation in obese subjects

Within the obese cohort, fifteen individuals underwent bariatric surgery for clinical purposes. Intra-operatory liver biopsy was performed for assessing the presence and severity of NAFLD and NASH; VAT samples were also collected for exploring the presence of AT inflammation and fibrosis. We demonstrated that, in obese subjects, lower BVR-A protein levels were associated with NASH ($r = -0.56$, $p = .03$) and with features of AT inflammation, as identified by greater UNC5B ($r = -0.60$, $p = .015$) and WISP1 ($r = -0.60$, $p = .02$) expression in VAT.

3.7. Increased BVR-A protein levels and improvement of insulin after bariatric surgery

Changes of BVR-A protein levels and insulin signaling pathway were assessed in PBMC collected from a subgroup of seven obese patients 6 months after bariatric surgery. BVR-A protein levels doubled after surgery ($p < .001$, Fig. 6B). IRS1 protein levels (~110%, $p = .02$, Fig. 6C), IRS1 activatory phosphorylation levels (~350%, $p = .007$, Fig. 6D) as well as relative IRS1 activation (~115%, $p = .01$, Fig. 6H) were significantly increased after intervention and these changes significantly associated with improved activation of the downstream targets. Indeed, we found a significant increase of Akt protein levels (~60%, $p = .04$, Fig. 7B) and Akt activatory phosphorylation (~40%, $p = .05$, Fig. 7C) in obese patients after bariatric surgery, along with a decrease of Akt relative activation, which returned comparable to the one measured in lean controls (Fig. 7D). Downstream Akt, recovered GSK-3β activatory phosphorylation (~80%, $p = .0002$, Fig. 7E) was observed, without changes of GSK-3β protein levels, finally resulting in an amelioration of the GSK-3β Tyr216/Ser9 ratio (~80%, $p = .02$, Fig. 7L). Furthermore, in this subgroup of patients we observed a reduction of AS160 protein levels (~50%, $p = .04$, Fig. 7M) and a

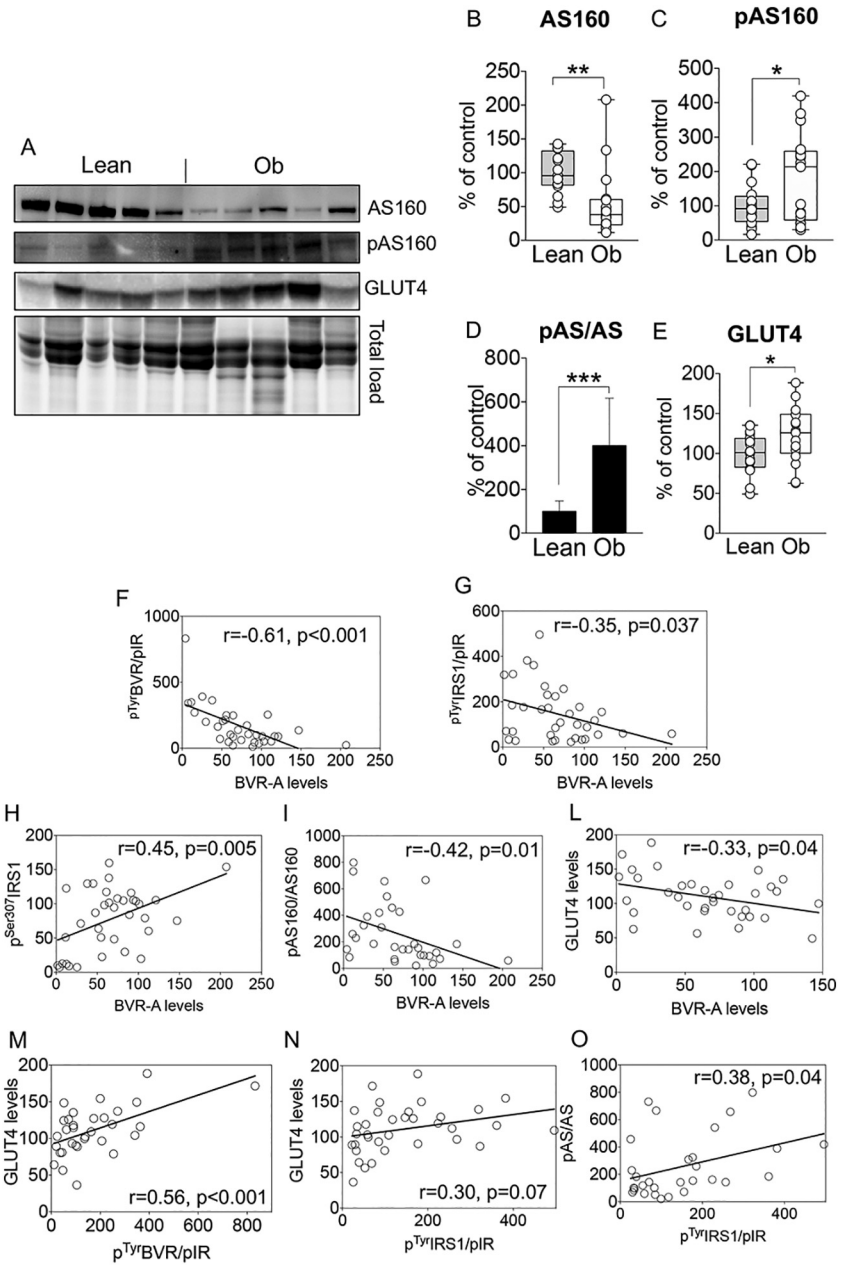

Fig. 4. Increased GLUT4 translocation at the plasma membrane in PBMC from obese individuals. (A) Western blot from lean and obese (Ob) individuals PBMC extracts. Representative gels are shown; (B) densitometric evaluation of AS160 protein levels; (C) densitometric evaluation of p^{Thr642}AS160 levels; (D) AS160 relative activation expressed as p^{Thr642}AS160/AS160 ratio; (E) densitometric evaluation of GLUT4 protein levels. Both total protein levels and respective phosphorylated forms were normalized per total protein load. Densitometric values are given as percentage of lean controls set as 100%. Data are presented as means ± SD (n = 20/group). *t*-test, *p < .05, ***p < .001. BVR-A protein levels correlate with (F) IR-mediated BVR-A activation, (G) IR-mediated IRS1 activation, (H) p^{Ser307}IRS1 levels, (I) AS160 relative activation, (L) GLUT4 protein levels. (M) IR-mediated BVR-A activation correlates with GLUT4 protein levels. (N) IR-mediated IRS1 activation correlates with GLUT4 protein levels. (M) IR-mediated IRS1 activation correlates with AS160 relative activation.

reduction of AS160 active form levels (~110%, p = .02, Fig. 7N), without significant changes of the relative AS160 activation (Fig. 7O). No changes of GLUT4 protein levels were observed (Fig. 7P).

4. Discussion

In this study, we provide evidence for the first time in humans that obese subjects show a consistent reduction of BVR-A protein levels compared to lean individuals and that impairment of BVR-A parallels the hyper-activation of the insulin signaling pathway in PBMC. Moreover, in obese subjects low BVR-A protein levels in PBMC correlate with the presence of MS, NAFLD and VAT inflammation.

Our hypothesis is consistent with the idea that reduced BVR-A protein levels represent an early alteration of insulin cascade that might precede the reduction of IR protein levels/activation and the inhibition of IRS1, which are two well-known molecular features of insulin-resistance [36,37,41].

Intriguingly, findings presented in the current study resemble what we previously observed in the brain from a mouse model of Alzheimer's disease [15,16], showing two age-associated phases: an early phase characterized by reduced BVR-A protein levels and activation together with the hyper-activation of the IR/IRS1 axis; and a late phase where the persistent impairment of BVRA is associated with inhibition of IRS1 and the onset of brain insulin resistance [15,16]. Indeed, we proposed that the hyper-activation of IRS1 represents a signal triggering the activation of feed-back mechanisms aimed to turn-off IRS1 hyper-activity and thus leading to brain insulin resistance [15,16]. The existence of these two phases is supported by *in vitro* studies showing that insulin treatment (100 sμM) increased glucose uptake in the short period (after 15–30 min) [10], while insulin led to insulin resistance development after 2 h [15,16], in HEK cells knocked-down for BVR-A. Nevertheless, insulin activation could be retrieved following a co-administration of insulin with a BVR-A mimetic peptide, in the same cells [16].

Reduced BVR-A protein levels in obese subjects could be dependent on an impaired transcription process since reduced BVR-A mRNA levels were observed in PBMC. Among the known BVR-A transcriptional regulators, biliverdin (the end-product of HO enzymatic activity [5]) and NF-kB play a pivotal role [42]. In particular, NF-kB strongly

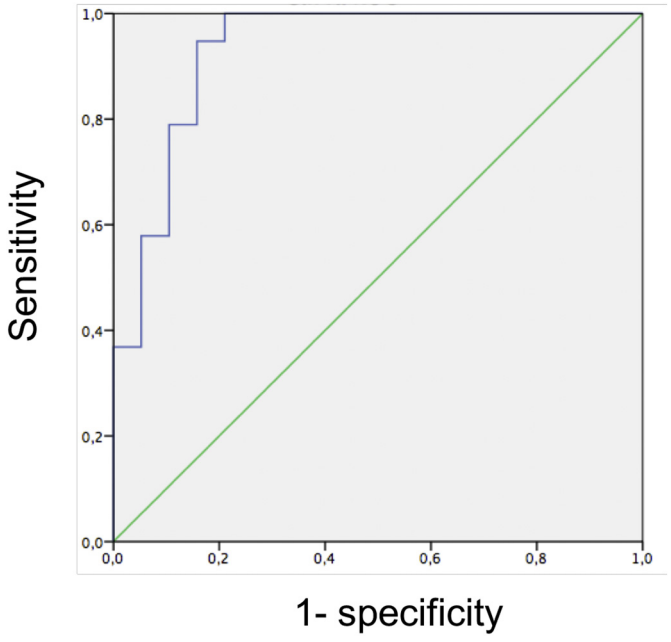

Fig. 5. BVR-A ROC curve for obesity.

inhibits BVR-A transcription, while biliverdin suppresses the inhibitory effects of NF-kB [42]. Furthermore, BVR-A-mediated biliverdin conversion to bilirubin was shown to increase p^{Tyr198}BVR-A levels [43]. Considering that reduced HO levels/activity were observed in humans and experimental models of metabolic disorders [44–50] (also in PBMC [51–53]), it would be conceivable to hypothesize that reduced HO-mediated production of biliverdin would from one side lead to reduced BVR-A gene transcription and from another side might contribute to reduced p^{Tyr198}BVR-A, which finally impact on insulin signaling activation. However, this is an interesting aspect, which was out of the scope of this paper and will be certainly addressed in future studies.

In obese subjects, the hypothesis of an influence exerted by BVR-A on the insulin signaling pathway is supported by the observation that the net hyper-activation of IRS1 seems to be not dependent on IR. Indeed, we did not observe changes of either IR or p^{Tyr632}IRS1 (the active isoform); rather, the significant decrease of p^{Ser307}IRS1 (the inhibited isoform), may indicate the loss of BVR-A regulatory control [5,10,12]. This is further consistent with the notion that while IRS1 Ser307 phosphorylation can increase following the aberrant activation of kinases, *i.e.*, mTOR, S6K, JNK (known to be involved in the development of insulin resistance) [36,41,54], the opposite it is unlikely to happen, thus reinforcing the idea about a possible direct involvement of BVR-A in the observed reduced IRS1 Ser307 phosphorylation [5,10,15,16]. In agreement, no changes have been found about mTOR activation in PBMC collected from obese subjects with respect to lean controls.

IRS1 hyper-activation has effects downstream, as showed by the increased Akt activation (p^{Ser473}Akt/Akt ratio), which mediates the inhibition of GSK-3β (increased p^{Ser9}GSK-3β/GSK-3β ratio) as well as the increase of AS160-mediated GLUT4 translocation at the plasma

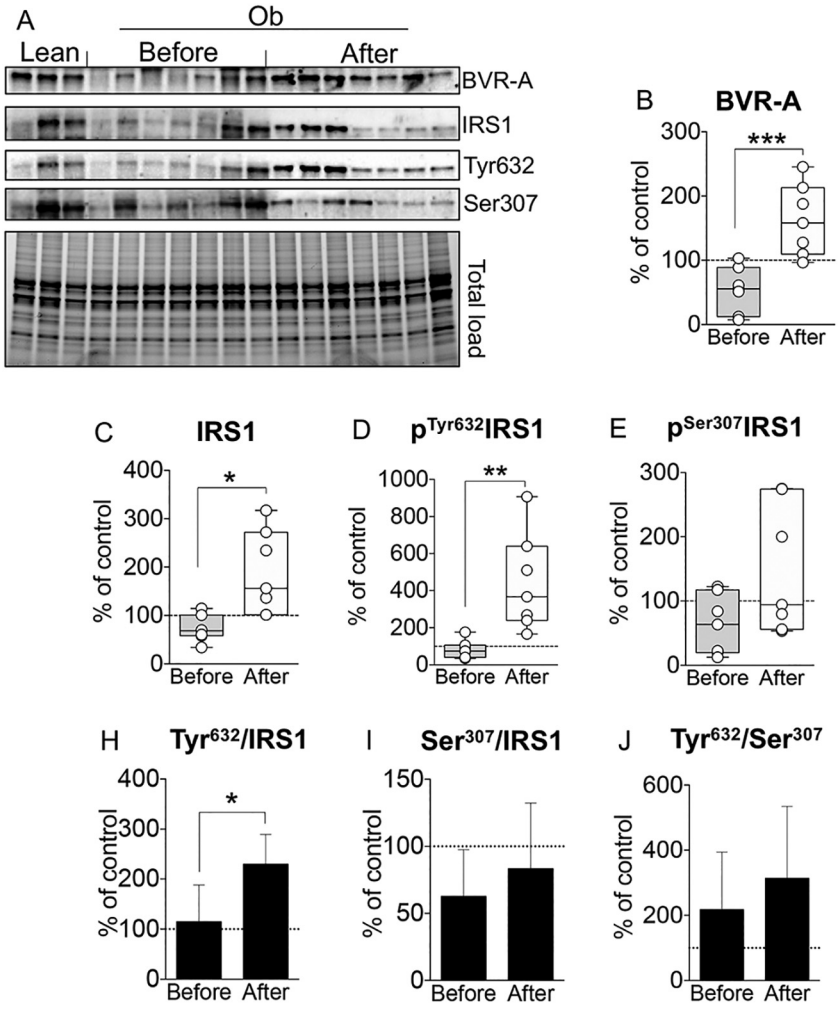

Fig. 6. Increased BVR-A protein levels and improved IRS1 activation in PBMC from obese individuals after bariatric surgery. (A) Western blot from lean and obese (Ob) individuals PBMC extracts. Representative gels are shown; (B) densitometric evaluation of BVR-A protein levels; (C) densitometric evaluation of IRS1 protein levels; (D) densitometric evaluation of p^{Tyr632}IRS1 levels; (E) densitometric evaluation of p^{Ser307}IRS1 levels; (F) IRS1 relative activation evaluated as p^{Tyr632}IRS1/IRS1 ratio; (G) IRS1 relative inactivation evaluated as p^{Ser307}IRS1/IRS1; (H) IRS1 activation/inactivation ratio evaluated as (p^{Tyr632}IRS1/IRS1)/(p^{Ser307}IRS1/IRS1). Both total protein levels and respective phosphorylated forms were normalized per total protein load. Densitometric values are given as percentage of lean controls set as 100%. Data are presented as means ± SD (n = 7/group). *t*-test, *p < .05, ***p < .001.

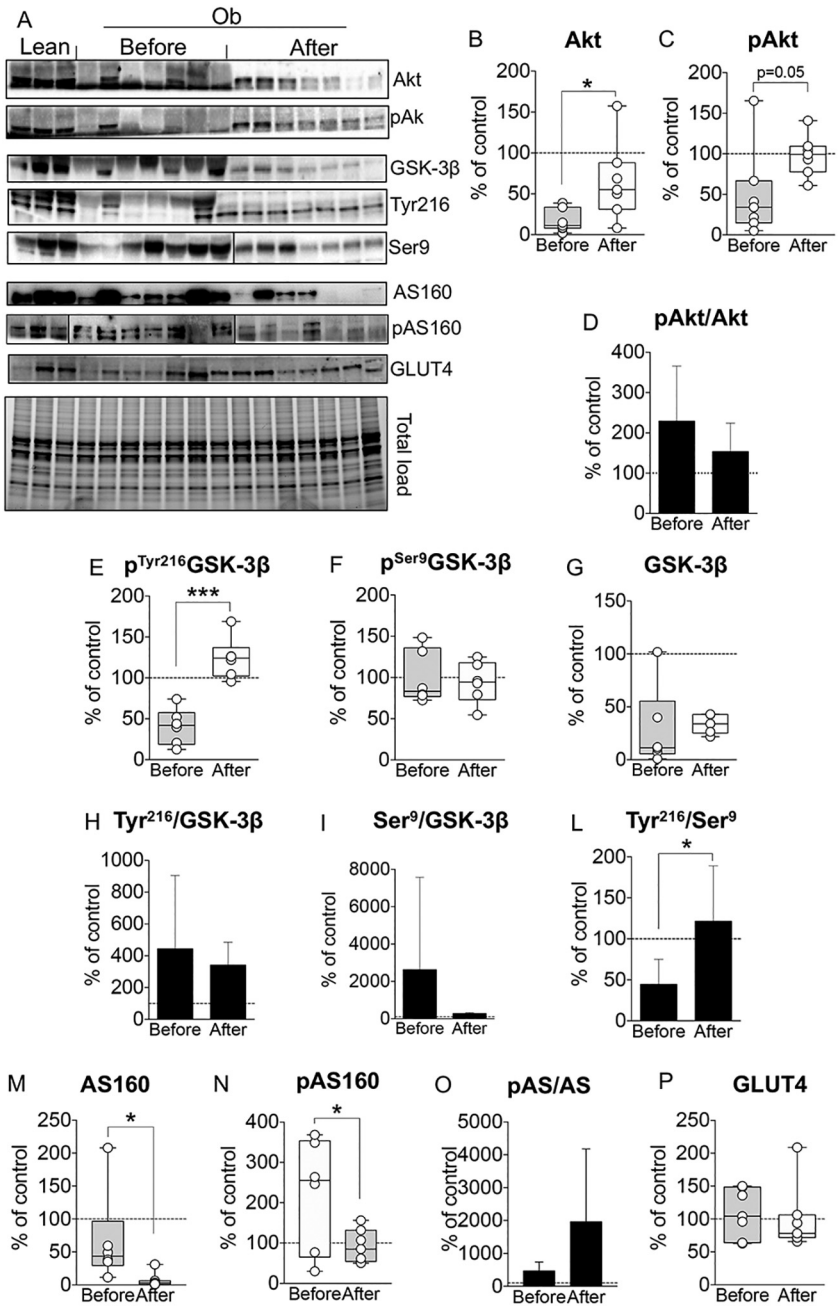

Fig. 7. Improved Akt activation and downstream pathways in PBMC from obese individuals after bariatric surgery. (A) Western blot from lean and obese (Ob) individuals PBMC extracts. Representative gels are shown; (B) densitometric evaluation of Akt protein levels; (C) densitometric evaluation of p^{Ser473}Akt levels; (D) Akt relative activation expressed as p^{Ser473}Akt/Akt ratio; (E) densitometric evaluation of GSK-3β protein levels; (F) densitometric evaluation of p^{Tyr216}GSK-3β levels; (G) densitometric evaluation of p^{Ser9} GSK-3β levels; (H) GSK-3β relative activation evaluated as p^{Tyr216}GSK-3β/GSK-3β ratio; (I) GSK-3β relative inactivation evaluated as p^{Ser9}GSK-3β/GSK-3β; (L) GSK-3β activation/inactivation ratio evaluated as (p^{Tyr216}GSK-3β/GSK-3β)/(p^{Ser9}GSK-3β/GSK-3β); (M) densitometric evaluation of AS160 protein levels; (N) densitometric evaluation of p^{Thr642}AS160 levels; (O) AS160 relative activation expressed as p^{Thr642}AS160/AS160 ratio; (P) densitometric evaluation of GLUT4 protein levels. Both total protein levels and respective phosphorylated forms were normalized per total protein load. Densitometric values are given as percentage of lean controls set as 100%. Data are presented as means ± SD (n = 7/group). *t*-test, *p < .05, ***p < .001.

membrane (increased p^{Thr642}AS160/AS160 ratio). Hence, observed changes in the relative activation of each protein suggest that despite reduced total protein levels (*i.e.*, for IRS1, Akt, GSK-3β and AS160) the residual proteins are increasingly activated/inhibited to such a level as to be capable of compensating for reduced amount of protein. Except for BVR-A, whose increased relative activation (p^{Tyr198}BVR-A/BVR-A ratio) is not associated with a parallel increase of IRS1 Ser307 phosphorylation.

Our obese population showed normal glucose and insulin levels before and after OGTT and no alterations of indexes of insulin resistance and secretion. Intriguingly, reduced BVR-A levels correlate with higher blood glucose in the course of OGTT, although within physiological ranges, and positively associated with DI, which estimates the insulin secretory capacity adjusted for insulin resistance [20], and with CIR30, an index estimating beta cells secretion [21]. Conversely, no association was found between BVR-A protein levels and index of insulin resistance such as HOMA-IR or ISI. Several explanations can be called upon to explain this lack of correlation. These indexes are not accurate indicators of insulin resistance in small samples and are normally used in large epidemiological studies. For this reason, the correlation with overt insulin resistance did not represent an endpoint of this study, which indeed was not powered to explore this aspect. Furthermore, we are aware that despite PBMC are increasingly used as surrogate model for glucose disposal [25–29], they likely do not perfectly reflect changes occurring in the main tissues for insulin-dependent glucose metabolism such as liver or skeletal muscles, thus representing a limitation of our study. Notwithstanding, the use of PBMC is of help to perform studies aimed to compare changes in obese subjects with respect to matched controls, which otherwise would not be possible.

The significant correlations found between BVR-A and metabolic indexes, might therefore suggest that the hyper-activation of insulin, along with increased GLUT4 expression and translocation may preserve the euglycaemic state without increasing insulin secretion. Hence, BVR-

A impairment may, at the beginning, be responsible for the hyper-activation of insulin, providing an early contribution to the maintenance of a normal glucose regulation, whereas it may lead to the development of insulin resistance later on. Indeed, in obese subjects low BVR-A levels are negatively associated with a peculiar clinical phenotype characterized by the presence of metabolic syndrome, NAFLD and adipose tissue inflammation, which are aspects closely associated to insulin-resistance.

Related to the above-cited data, a role for bilirubin – the end-product of BVR-A enzymatic activity [5] – in protecting from the development of NAFLD or NASH was proposed (reviewed in [7,55–58]). Several studies in diverse human patient populations, and experimental investigations in rodents, have demonstrated the protective effects of hyperbilirubinemia in preventing both the development of chronic liver disease [59–62] and obesity [7,18,59,62–64]. Bilirubin would exert its protective functions by activating the peroxisome proliferator-activated receptor-α (PPARα) that is ultimately responsible for the uptake, utilization and catabolism of fatty acids though the upregulation of genes involved in fatty acid transport and peroxisomal and mitochondrial fatty acid β-oxidation [18,59,62]. Hence, reduced BVR-A protein levels would also lead to reduced bilirubin production finally favoring the development of NAFLD and NASH in obese subjects.

Furthermore, results presented in the current study agree with previous observations collected *in vitro* [10,15,17,18] as well as in liver-specific BVR-A KO mice fed high fat diet, which were characterized by significant alterations of fasting plasma glucose, insulin levels, hepatic lipid accumulation and reduced p^{Ser473}Akt/Akt and p^{Ser9}GSK-3β/GSK-3β ratios, thus indicating a condition of insulin resistance [18].

In addition, it is interesting that in a sub-group consisting of 7 subjects who underwent bariatric surgery and that were re-evaluated 6 months after the operation, we observed a recovery of BVR-A levels along with an improved insulin sensitivity. Indeed, while the hyper-activation of the insulin signaling pathway was mainly driven by the reduction of p^{Ser307}IRS1 (the inhibited isoform), we observed an increased activation of IRS1 (p^{Tyr632}IRS1) after bariatric surgery, that might suggest an improved response to insulin [36,37] in agreement with others [65–67]. This is coupled with an improved regulation of Akt activation as demonstrated by the levels of p^{Tyr216}GSK-3β (activatory), which return close to that of lean controls. In parallel, after 6 months from bariatric surgery these patients show no net changes in the activation of AS160 (p^{Thr642}AS160/AS160), although this likely due to a drop in the AS160 levels compensated by the levels of the active form of the protein (p^{Thr642}AS160). This result agrees with previous findings in muscles and adipose tissue [68,69] suggesting that Akt still sustains the processes mediating GLUT4 translocation required for glucose uptake. However, after bariatric surgery the effect seems preferably to be the result of an improved insulin response rather than a hyper-active signal. These data, although derived from a small sample, may support the association between the alteration of BVR-A with obesity, metabolic syndrome and insulin resistance, given that bariatric surgery is an effective therapy for these diseases [70].

Finally, we acknowledge that the cross-sectional design of our study does not allow us to establish with certainty a causal nexus between BVR-A impairment, insulin signaling pathway deregulation and metabolic complications of obesity. However, this is the first study to highlight the potential role of BVR-A in the regulation of the insulin signaling pathway in humans, suggesting that an impairment of BVR-A may represent an early alteration in the process of insulin-resistance development. Further studies are warranted for fully understanding the pathophysiologic processes behind our observations and the possible clinical implications.

5. Conclusions

In summary, our study show for the first time in humans that BVR-A protein levels and activation are reduced in obesity and are associated with impaired insulin signaling and metabolic disease. The overall data add insights to the mechanisms underlying metabolic alterations in obesity and may open new tracks for innovative therapeutic approaches to obesity prevention and care.

Conflict of interest

The authors declare that they have no conflict of interest

Transparency document

The Transparency document associated with this article can be found, in online version

Acknowledgements

This work was supported by Fondi Ateneo grant funded by Sapienza University of Romes n° RM11715C77336E99 to EB; by funding from Banca d'Italia n° 12868/17 to EB; by Fondi Ateneo grant funded by Sapienza University of Rome n° C26H15JT9X MP; Fondi Ateneo grant funded by Sapienza University of Rome n° RM116155s0687D69B (MGC).

Author contribution

EB and MGC conceived the study; EB, MP, MGC, MF, IB and FAC participated to study design; FL, DC, FAC, IB, VC and LB enrolled the subjects, performed the clinical evaluation and collected the samples; GS performed surgery; AA, AT, CL and FDD performed the biochemical analyses; CDC and CC performed histology and molecular biology on tissue biopsies; VC, FAC, IB and EB prepared the databases; EB, MGC, FAC, IB, MP analyzed and interpreted the data; EB, MGC, MGB, MP drafted the manuscript.

All authors revised the manuscript critically for important intellectual content and approved the final version

References

[1] L.F. Van Gaal, A.P. Maggioni, Overweight, obesity, and outcomes: fat mass and beyond, Lancet 383 (2014) 935–936.
[2] B.C. Lee, J. Lee, Cellular and molecular players in adipose tissue inflammation in the development of obesity-induced insulin resistance, Biochim. Biophys. Acta 1842 (2014) 446–462.
[3] J. Ye, Mechanisms of insulin resistance in obesity, Front Med 7 (2013) 14–24.
[4] C.M. Taniguchi, B. Emanuelli, C.R. Kahn, Critical nodes in signalling pathways: insights into insulin action, Nat Rev Mol Cell Biol 7 (2006) 85–96.
[5] J. Kapitulnik, M.D. Maines, Pleiotropic functions of biliverdin reductase: cellular signaling and generation of cytoprotective and cytotoxic bilirubin, Trends Pharmacol. Sci. 30 (2009) 129–137.
[6] E. Barone, F. Di Domenico, C. Mancuso, D.A. Butterfield, The Janus face of the heme oxygenase/biliverdin reductase system in Alzheimer disease: it's time for reconciliation, Neurobiol. Dis. 62 (2014) 144–159.
[7] L. O'Brien, P.A. Hosick, K. John, D.E. Stec, T.D. Hinds Jr., Biliverdin reductase isozymes in metabolism, Trends Endocrinol. Metab. 26 (2015) 212–220.
[8] U.M. Florczyk, A. Jozkowicz, J. Dulak, Biliverdin reductase: new features of an old enzyme and its potential therapeutic significance, Pharmacol. Rep. 60 (2008) 38–48.
[9] W. Chen, G.J. Maghzal, A. Ayer, C. Suarna, L.L. Dunn, R. Stocker, Absence of the biliverdin reductase-a gene is associated with increased endogenous oxidative stress, Free Radic. Biol. Med. 115 (2018) 156–165.
[10] N. Lerner-Marmarosh, J. Shen, M.D. Torno, A. Kravets, Z. Hu, M.D. Maines, Human biliverdin reductase: a member of the insulin receptor substrate family with serine/threonine/tyrosine kinase activity, Proc. Natl. Acad. Sci. U. S. A. 102 (2005) 7109–7114.
[11] P.E. Gibbs, N. Lerner-Marmarosh, A. Poulin, E. Farah, M.D. Maines, Human biliverdin reductase-based peptides activate and inhibit glucose uptake through direct interaction with the kinase domain of insulin receptor, FASEB J. 28 (2014) 2478–2491.
[12] T. Miralem, N. Lerner-Marmarosh, P.E. Gibbs, J.L. Jenkins, C. Heimiller, M.D. Maines, Interaction of human biliverdin reductase with Akt/protein kinase B and phosphatidylinositol-dependent kinase 1 regulates glycogen synthase kinase 3 activity: a novel mechanism of Akt activation, FASEB J. 30 (2016) 2926–2944.
[13] P.E. Gibbs, T. Miralem, N. Lerner-Marmarosh, C. Tudor, M.D. Maines, Formation of ternary complex of human biliverdin reductase-protein kinase Cdelta-ERK2 protein

is essential for ERK2-mediated activation of Elk1 protein, nuclear factor-kappaB, and inducible nitric-oxidase synthase (iNOS), J. Biol. Chem. 287 (2012) 1066–1079.
[14] N. Lerner-Marmarosh, T. Miralem, P.E. Gibbs, M.D. Maines, Human biliverdin reductase is an ERK activator; hBVR is an ERK nuclear transporter and is required for MAPK signaling, Proc. Natl. Acad. Sci. U. S. A. 105 (2008) 6870–6875.
[15] E. Barone, F. Di Domenico, T. Cassano, A. Arena, A. Tramutola, M.A. Lavecchia, R. Coccia, D.A. Butterfield, M. Perluigi, Impairment of biliverdin reductase-a promotes brain insulin resistance in Alzheimer disease: a new paradigm, Free Radic. Biol. Med. 91 (2016) 127–142.
[16] E. Barone, A. Tramutola, F. Triani, S. Calcagnini, F. Di Domenico, C. Ripoli, S. Gaetani, C. Grassi, D.A. Butterfield, T. Cassano, M. Perluigi, Biliverdin reductase-a mediates the beneficial effects of intranasal insulin in Alzheimer disease, Mol. Neurobiol. (2018), https://doi.org/10.1007/s1203.
[17] S.O. Adeosun, D.M. Gordon, M.F. Weeks, K.H. Moore, J.E. Hall, T.D. Hinds, D.E. Stec, Loss of biliverdin reductase-A (BVRA) promotes lipid accumulation and lipotoxicity in mouse proximal tubule cells, Am J Physiol Renal Physiol 315 (2) (2018) F323–F331, https://doi.org/10.1152/ajprenal.00495.2017.
[18] T.D. Hinds Jr., K.A. Burns, P.A. Hosick, L. McBeth, A. Nestor-Kalinoski, H.A. Drummond, A.A. AlAmodi, M.W. Hankins, J.P. Vanden Heuvel, D.E. Stec, Biliverdin reductase a attenuates hepatic steatosis by inhibition of glycogen synthase kinase (GSK) 3beta phosphorylation of serine 73 of peroxisome proliferator-activated receptor (PPAR) alpha, J. Biol. Chem. 291 (2016) 25179–25191.
[19] M. Matsuda, R.A. DeFronzo, Insulin sensitivity indices obtained from oral glucose tolerance testing: comparison with the euglycemic insulin clamp, Diabetes Care 22 (1999) 1462–1470.
[20] S.A. Herzberg-Schafer, H. Staiger, M. Heni, C. Ketterer, M. Guthoff, K. Kantartzis, F. Machicao, N. Stefan, H.U. Haring, A. Fritsche, Evaluation of fasting state−/oral glucose tolerance test-derived measures of insulin release for the detection of genetically impaired beta-cell function, PLoS One 5 (2010) e14194.
[21] R.N. Bergman, M. Ader, K. Huecking, G. Van Citters, Accurate assessment of beta-cell function: the hyperbolic correction, Diabetes 51 (Suppl. 1) (2002) S212–S220.
[22] D.E. Kleiner, E.M. Brunt, Nonalcoholic fatty liver disease: pathologic patterns and biopsy evaluation in clinical research, Semin. Liver Dis. 32 (2012) 3–13.
[23] D.E. Kleiner, E.M. Brunt, M. Van Natta, C. Behling, M.J. Contos, O.W. Cummings, L.D. Ferrell, Y.C. Liu, M.S. Torbenson, A. Unalp-Arida, M. Yeh, A.J. McCullough, A.J. Sanyal, N. Nonalcoholic Steatohepatitis Clinical Research, Design and validation of a histological scoring system for nonalcoholic fatty liver disease, Hepatology 41 (2005) 1313–1321.
[24] I. Barchetta, F.A. Cimini, D. Capoccia, L. Bertoccini, V. Ceccarelli, C. Chiappetta, F. Leonetti, C. Di Cristofano, G. Silecchia, M. Orho-Melander, O. Melander, M.G. Cavallo, Neurotensin is a lipid-induced gastrointestinal peptide associated with visceral adipose tissue inflammation in obesity, Nutrients 10 (2018).
[25] E. Maratou, G. Dimitriadis, A. Kollias, E. Boutati, V. Lambadiari, P. Mitrou, S.A. Raptis, Glucose transporter expression on the plasma membrane of resting and activated white blood cells, Eur. J. Clin. Investig. 37 (2007) 282–290.
[26] G. Dimitriadis, E. Maratou, E. Boutati, K. Psarra, C. Papasteriades, S.A. Raptis, Evaluation of glucose transport and its regulation by insulin in human monocytes using flow cytometry, Cytometry A 64 (2005) 27–33.
[27] E. Maratou, D.J. Hadjidakis, A. Kollias, K. Tsegka, M. Peppa, M. Alevizaki, P. Mitrou, V. Lambadiari, E. Boutati, D. Nikzas, N. Tountas, T. Economopoulos, S.A. Raptis, G. Dimitriadis, Studies of insulin resistance in patients with clinical and subclinical hypothyroidism, Eur. J. Endocrinol. 160 (2009) 785–790.
[28] P. Piatkiewicz, A. Czech, J. Taton, A. Gorski, Investigations of cellular glucose transport and its regulation under the influence of insulin in human peripheral blood lymphocytes, Endokrynol Pol 61 (2010) 182–187.
[29] A. Czech, P. Piatkiewicz, J. Taton, Cellular glucose transport and glucotransporter 4 expression as a therapeutic target: clinical and experimental studies, Arch. Immunol. Ther. Exp. 57 (2009) 467–473.
[30] I. Subhanova, L. Muchova, M. Lenicek, H.J. Vreman, O. Luksan, K. Kubickova, M. Kreidlova, T. Zima, L. Vitek, P. Urbanek, Expression of Biliverdin Reductase A in peripheral blood leukocytes is associated with treatment response in HCV-infected patients, PLoS One 8 (2013) e57555.
[31] M.L. Jison, P.J. Munson, J.J. Barb, A.F. Suffredini, S. Talwar, C. Logun, N. Raghavachari, J.H. Beigel, J.H. Shelhamer, R.L. Danner, M.T. Gladwin, Blood mononuclear cell gene expression profiles characterize the oxidant, hemolytic, and inflammatory stress of sickle cell disease, Blood 104 (2004) 270–280.
[32] V.D. de Mello, M. Kolehmainen, L. Pulkkinen, U. Schwab, U. Mager, D.E. Laaksonen, L. Niskanen, H. Gylling, M. Atalay, R. Rauramaa, M. Uusitupa, Downregulation of genes involved in NFkappaB activation in peripheral blood mononuclear cells after weight loss is associated with the improvement of insulin sensitivity in individuals with the metabolic syndrome: the GENOBIN study, Diabetologia 51 (2008) 2060–2067.
[33] V.D. de Mello, M. Kolehmainen, U. Schwab, U. Mager, D.E. Laaksonen, L. Pulkkinen, L. Niskanen, H. Gylling, M. Atalay, R. Rauramaa, M. Uusitupa, Effect of weight loss on cytokine messenger RNA expression in peripheral blood mononuclear cells of obese subjects with the metabolic syndrome, Metabolism 57 (2008) 192–199.
[34] H. Ghanim, A. Aljada, D. Hofmeyer, T. Syed, P. Mohanty, P. Dandona, Circulating mononuclear cells in the obese are in a proinflammatory state, Circulation 110 (2004) 1564–1571.
[35] K.J. Livak, T.D. Schmittgen, Analysis of relative gene expression data using real-time quantitative PCR and the 2(−Delta Delta C(T)) method, Methods 25 (2001) 402–408.
[36] K.D. Copps, M.F. White, Regulation of insulin sensitivity by serine/threonine phosphorylation of insulin receptor substrate proteins IRS1 and IRS2, Diabetologia 55 (2012) 2565–2582.
[37] R.A. Haeusler, T.E. McGraw, D. Accili, Biochemical and cellular properties of insulin receptor signalling, Nat Rev Mol Cell Biol 19 (2018) 31–44.
[38] M.A. Hermida, J. Dinesh Kumar, N.R. Leslie, GSK3 and its interactions with the PI3K/AKT/mTOR signalling network, Adv Biol Regul 65 (2017) 5–15.
[39] A. Ardestani, B. Lupse, Y. Kido, G. Leibowitz, K. Maedler, mTORC1 signaling: a double-edged sword in diabetic beta cells, Cell Metab. 27 (2018) 314–331.
[40] J.S. Bogan, Regulation of glucose transporter translocation in health and diabetes, Annu. Rev. Biochem. 81 (2012) 507–532.
[41] S. Guo, Insulin signaling, resistance, and the metabolic syndrome: insights from mouse models into disease mechanisms, J. Endocrinol. 220 (2014) T1–T23.
[42] P.E. Gibbs, M.D. Maines, Biliverdin inhibits activation of NF-kappaB: reversal of inhibition by human biliverdin reductase, Int. J. Cancer 121 (2007) 2567–2574.
[43] B. Wegiel, C.J. Baty, D. Gallo, E. Csizmadia, J.R. Scott, A. Akhavan, B.Y. Chin, E. Kaczmarek, J. Alam, F.H. Bach, B.S. Zuckerbraun, L.E. Otterbein, Cell surface biliverdin reductase mediates biliverdin-induced anti-inflammatory effects via phosphatidylinositol 3-kinase and Akt, J. Biol. Chem. 284 (2009) 21369–21378.
[44] A.L. Kruger, S.J. Peterson, M.L. Schwartzman, H. Fusco, J.A. McClung, M. Weiss, S. Shenouda, A.I. Goodman, M.S. Goligorsky, A. Kappas, N.G. Abraham, Up-regulation of heme oxygenase provides vascular protection in an animal model of diabetes through its antioxidant and antiapoptotic effects, J. Pharmacol. Exp. Ther. 319 (2006) 1144–1152.
[45] N.G. Abraham, T. Kushida, J. McClung, M. Weiss, S. Quan, R. Lafaro, Z. Darzynkiewicz, M. Wolin, Heme oxygenase-1 attenuates glucose-mediated cell growth arrest and apoptosis in human microvessel endothelial cells, Circ. Res. 93 (2003) 507–514.
[46] S.H. Chang, J. Garcia, J.A. Melendez, M.S. Kilberg, A. Agarwal, Haem oxygenase 1 gene induction by glucose deprivation is mediated by reactive oxygen species via the mitochondrial electron-transport chain, Biochem. J. 371 (2003) 877–885.
[47] S.H. Chang, I. Barbosa-Tessmann, C. Chen, M.S. Kilberg, A. Agarwal, Glucose deprivation induces heme oxygenase-1 gene expression by a pathway independent of the unfolded protein response, J. Biol. Chem. 277 (2002) 1933–1940.
[48] D. Sacerdoti, S.P. Singh, J. Schragenheim, L. Bellner, L. Vanella, M. Raffaele, A. Meissner, I. Grant, G. Favero, R. Rezzani, L.F. Rodella, D. Bamshad, E. Lebovics, N.G. Abraham, Development of NASH in obese mice is confounded by adipose tissue increase in inflammatory NOV and oxidative stress, Int J Hepatol 2018 (2018) 3484107.
[49] N.G. Abraham, J.M. Junge, G.S. Drummond, Translational significance of heme oxygenase in obesity and metabolic syndrome, Trends Pharmacol. Sci. 37 (2016) 17–36.
[50] C.R. Bruce, A.L. Carey, J.A. Hawley, M.A. Febbraio, Intramuscular heat shock protein 72 and heme oxygenase-1 mRNA are reduced in patients with type 2 diabetes: evidence that insulin resistance is associated with a disturbed antioxidant defense mechanism, Diabetes 52 (2003) 2338–2345.
[51] F. Song, X. Li, M. Zhang, P. Yao, N. Yang, X. Sun, F.B. Hu, L. Liu, Association between heme oxygenase-1 gene promoter polymorphisms and type 2 diabetes in a Chinese population, Am. J. Epidemiol. 170 (2009) 747–756.
[52] C. Mozzini, U. Garbin, C. Stranieri, A. Pasini, E. Solani, I.A. Tinelli, L. Cominacini, A.M. Fratta Pasini, Endoplasmic reticulum stress and Nrf2 repression in circulating cells of type 2 diabetic patients without the recommended glycemic goals, Free Radic. Res. 49 (2015) 244–252.
[53] F.F. Mahmoud, D. Haines, A.A. Dashti, S. El-Shazly, F. Al-Najjar, Correlation between heat shock proteins, adiponectin, and T lymphocyte cytokine expression in type 2 diabetics, Cell Stress Chaperones 23 (2018) 955–965.
[54] M.S. Yoon, The role of mammalian target of rapamycin (mTOR) in insulin signaling, Nutrients 9 (2017).
[55] T.D. Hinds Jr., S.O. Adeosun, A.A. Alamodi, D.E. Stec, Does bilirubin prevent hepatic steatosis through activation of the PPARalpha nuclear receptor? Med. Hypotheses 95 (2016) 54–57.
[56] T.D. Hinds Jr., D.E. Stec, Bilirubin, a Cardiometabolic signaling molecule, Hypertension 72 (2018) 788–795.
[57] L. Weaver, A.R. Hamoud, D.E. Stec, T.D. Hinds Jr., Biliverdin reductase and bilirubin in hepatic disease, Am. J. Physiol. Gastrointest. Liver Physiol. 314 (2018) G668–G676.
[58] A.R. Hamoud, L. Weaver, D.E. Stec, T.D. Hinds Jr., Bilirubin in the liver-gut signaling axis, Trends Endocrinol. Metab. 29 (2018) 140–150.
[59] D.E. Stec, K. John, C.J. Trabbic, A. Luniwal, M.W. Hankins, J. Baum, T.D. Hinds Jr., Bilirubin binding to PPARalpha inhibits lipid accumulation, PLoS One 11 (2016) e0153427.
[60] B.K. Jang, Elevated serum bilirubin levels are inversely associated with nonalcoholic fatty liver disease, Clin Mol Hepatol 18 (2012) 357–359.
[61] M.S. Kwak, D. Kim, G.E. Chung, S.J. Kang, M.J. Park, Y.J. Kim, J.H. Yoon, H.S. Lee, Serum bilirubin levels are inversely associated with nonalcoholic fatty liver disease, Clin Mol Hepatol 18 (2012) 383–390.
[62] T.D. Hinds Jr., P.A. Hosick, S. Chen, R.H. Tukey, M.W. Hankins, A. Nestor-Kalinoski, D.E. Stec, Mice with hyperbilirubinemia due to Gilbert's syndrome polymorphism are resistant to hepatic steatosis by decreased serine 73 phosphorylation of PPARalpha, Am. J. Physiol. Endocrinol. Metab. 312 (2017) E244–E252.
[63] L. Belo, H. Nascimento, M. Kohlova, E. Bronze-da-Rocha, J. Fernandes, E. Costa, C. Catarino, L. Aires, H.F. Mansilha, P. Rocha-Pereira, A. Quintanilha, C. Rego, A. Santos-Silva, Body fat percentage is a major determinant of total bilirubin independently of UGT1A1*28 polymorphism in young obese, PLoS One 9 (2014) e98467.
[64] T.D. Hinds Jr., K. Sodhi, C. Meadows, L. Fedorova, N. Puri, D.H. Kim, S.J. Peterson, J. Shapiro, N.G. Abraham, A. Kappas, Increased HO-1 levels ameliorate fatty liver development through a reduction of heme and recruitment of FGF21, Obesity

(Silver Spring) 22 (2014) 705–712.
[65] B.T. Bikman, D. Zheng, W.J. Pories, W. Chapman, J.R. Pender, R.C. Bowden, M.A. Reed, R.N. Cortright, E.B. Tapscott, J.A. Houmard, C.J. Tanner, J. Lee, G.L. Dohm, Mechanism for improved insulin sensitivity after gastric bypass surgery, J. Clin. Endocrinol. Metab. 93 (2008) 4656–4663.
[66] S.Q. Li, Y. Zhou, Y. Wang, Y. Liu, D.H. Geng, J.G. Liu, Upregulation of IRS-1 expression in Goto-Kakizaki rats following Roux-en-Y gastric bypass surgery: resolution of type 2 diabetes? Tohoku J. Exp. Med. 225 (2011) 179–186.
[67] S. Bonhomme, A. Guijarro, S. Keslacy, C.G. Goncalves, S. Suzuki, C. Chen, M.M. Meguid, Gastric bypass up-regulates insulin signaling pathway, Nutrition 27 (2011) 73–80.
[68] P.H. Albers, K.N. Bojsen-Moller, C. Dirksen, A.K. Serup, D.E. Kristensen, J. Frystyk, T.R. Clausen, B. Kiens, E.A. Richter, S. Madsbad, J.F. Wojtaszewski, Enhanced insulin signaling in human skeletal muscle and adipose tissue following gastric bypass surgery, Am J Physiol Regul Integr Comp Physiol 309 (2015) R510–R524.
[69] J.M. Hinkley, K. Zou, S. Park, K. Turner, D. Zheng, J.A. Houmard, Roux-en-Y gastric bypass surgery enhances contraction-mediated glucose metabolism in primary human myotubes, Am. J. Physiol. Endocrinol. Metab. 313 (2017) E195–E202.
[70] A.R. Vest, H.M. Heneghan, P.R. Schauer, J.B. Young, Surgical management of obesity and the relationship to cardiovascular disease, Circulation 127 (2013) 945–959.